

Observation of the Decay $B_c^+ \rightarrow B_s^0 \pi^+$

R. Aaij *et al.**

(LHCb Collaboration)

(Received 22 August 2013; published 1 November 2013)

The result of a search for the decay $B_c^+ \rightarrow B_s^0 \pi^+$ is presented, using the $B_s^0 \rightarrow D_s^- \pi^+$ and $B_s^0 \rightarrow J/\psi \phi$ channels. The analysis is based on a data sample of pp collisions collected with the LHCb detector, corresponding to an integrated luminosity of 1 fb^{-1} taken at a center-of-mass energy of 7 TeV, and 2 fb^{-1} taken at 8 TeV. The decay $B_c^+ \rightarrow B_s^0 \pi^+$ is observed with significance in excess of 5 standard deviations independently in both decay channels. The measured product of the ratio of cross sections and branching fraction is $[\sigma(B_c^+)/\sigma(B_s^0)] \times \mathcal{B}(B_c^+ \rightarrow B_s^0 \pi^+) = [2.37 \pm 0.31 \text{ (stat)} \pm 0.11 \text{ (syst)}_{-0.13}^{+0.17} (\tau_{B_c^+})] \times 10^{-3}$, in the pseudorapidity range $2 < \eta(B) < 5$, where the first uncertainty is statistical, the second is systematic, and the third is due to the uncertainty on the B_c^+ lifetime. This is the first observation of a B meson decaying to another B meson via the weak interaction.

DOI: 10.1103/PhysRevLett.111.181801

PACS numbers: 13.25.Hw, 12.15.Ji

The B_c^+ meson is the ground state of the $\bar{b}c$ system. As such it is unique as it is the only weakly decaying doubly heavy meson. All measurements of B_c^+ meson decays to date are decays where the constituent b quark decays weakly to a c quark [1–8]. The decay of the B_c^+ meson to another B meson, with the bottom quark acting as a spectator (see Fig. 1), has not previously been observed. This will improve the understanding of theoretical predictions and provide valuable information for the source of B_s^0 mesons at the LHC.

A wide range of predictions for the branching fraction $\mathcal{B}(B_c^+ \rightarrow B_s^0 \pi^+)$ exists, between 16.4% and 2.5%, based on, e.g., QCD sum rules [9,10], or quark-potential models (see Refs. [11–16] and references therein). Experimental clarification is needed to shed light on the present theoretical status. Unlike most other B decays, the higher order corrections in the expansion of Heavy Quark Effective Theory within the framework of quantum chromodynamics (QCD) are relatively large. The expansion is described in powers of m_c/m_b rather than Λ_{QCD}/m_b , due to the presence of two heavy quark constituents, where Λ_{QCD} is the QCD scale, and m_c (m_b) the charm (bottom) quark mass. In addition, the energy release in the decay is relatively small, leading to larger nonfactorizable effects compared to decays with lighter daughter particles. Study of the decay $B_c^+ \rightarrow B_s^0 \pi^+$ allows these models to be tested. Knowledge of the production of B_s^0 mesons from B_c^+ decays is also useful for time-dependent analyses of B_s^0 decays, to understand any associated decay-time bias due to the incorrect estimate of the B_s^0 decay time if

originating from a B_c^+ decay, or to take advantage of flavor tagging capabilities using the accompanying (“bachelor”) pion.

The data used in this analysis were collected with the LHCb detector [17] from pp collisions at $\sqrt{s} = 7 \text{ TeV}$ and 8 TeV, corresponding to integrated luminosities of 1 fb^{-1} and 2 fb^{-1} , respectively.

The decays $B_s^0 \rightarrow D_s^- \pi^+$ and $B_s^0 \rightarrow J/\psi \phi$ are used, with the subsequent decays $D_s^- \rightarrow K^+ K^- \pi^-$, $J/\psi \rightarrow \mu^+ \mu^-$ and $\phi \rightarrow K^+ K^-$. The inclusion of charge conjugate modes is implied throughout. The event selection and fits to the B_s^0 invariant mass distributions follow previous LHCb analyses based on these B_s^0 decay modes [18,19]. The two channels are analyzed independently and the final results are combined. The strategy is to normalize the final number of $B_c^+ \rightarrow B_s^0 \pi^+$ decays to the number of B_s^0 decays, which gives a result for the $B_c^+ \rightarrow B_s^0 \pi^+$ branching fraction multiplied by the ratio of B_c^+ and B_s^0 production rates, $[\sigma(B_c^+)/\sigma(B_s^0)] \times \mathcal{B}(B_c^+ \rightarrow B_s^0 \pi^+)$. The B_c^+ signal

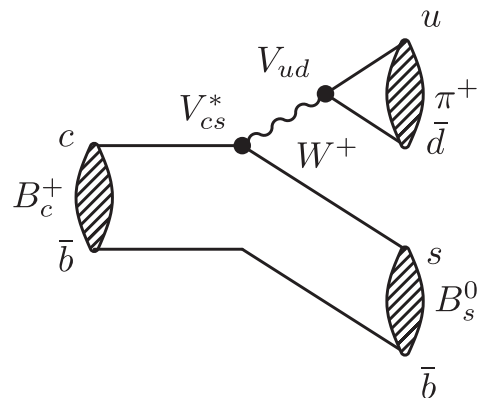


FIG. 1. Leading-order Feynman diagram of the decay $B_c^+ \rightarrow B_s^0 \pi^+$.

*Full author list given at end of the article.

Published by the American Physical Society under the terms of the [Creative Commons Attribution 3.0 License](https://creativecommons.org/licenses/by/3.0/). Further distribution of this work must maintain attribution to the author(s) and the published article's title, journal citation, and DOI.

region was not examined until the event selection was finalized. Since the ratio of production rates, $\sigma(B_c^+)/\sigma(B_s^0)$, may depend on the kinematics of the produced B meson, the result is quoted for B mesons produced in the pseudorapidity range $2 < \eta(B) < 5$, corresponding to the LHCb detector acceptance.

The LHCb detector is a single-arm forward spectrometer covering the pseudorapidity range $2 < \eta < 5$, described in detail in Ref. [17]. The combined tracking system provides momentum measurement with relative uncertainty that varies from 0.4% at 5 GeV/ c to 0.6% at 100 GeV/ c , and impact parameter resolution of 20 μm for tracks with high transverse momentum, p_T . The impact parameter (IP) is defined as the distance of closest approach between the track and a primary interaction. Charged hadrons are identified using two ring-imaging Cherenkov detectors. The charged pions from B_c^+ decays are selected with an efficiency of 93% while keeping the misidentification rate of kaons below 7%. Muons are identified by a system composed of alternating layers of iron and multiwire proportional chambers with a typical efficiency of 97% at 1%–3% pion to muon misidentification probability. The trigger [20] consists of a hardware stage, based on information from the calorimeter and muon systems, followed by a software stage, which applies a full event reconstruction. The B_s^0 candidates with muons in the final state are required to pass the hardware trigger, which selects muons with a transverse momentum, $p_T > 1.48$ GeV/ c , whereas the B_s^0 candidates with only hadrons in the final state are selected by requiring a hadron in the calorimeter with $E_T > 3.6$ GeV/ c .

Monte Carlo simulations, used to develop the B_c^+ candidate selection, are performed using BCVEGPY [21], interfaced with PYTHIA 6.4 [22] using a specific LHCb configuration [23]. Decays of hadronic particles are described by EVTGEN [24], in which final state radiation is generated using PHOTOS [25]. The interaction of the generated particles with the detector and its response are implemented using the GEANT4 toolkit [26] as described in Ref. [27].

The B_s^0 candidates are selected using the multivariate analysis known as the boosted decision tree (BDT) [28,29], to optimally discriminate between signal and background. In the training, simulated B_s^0 decays are used as the signal, whereas candidates in the B_s^0 mass sideband in data are used as the background. To avoid potential biases, only one sixth of the data is used in the training. It is verified that the distribution of the BDT discriminant is the same for the events used in the training, compared to those that were not. All events are used for the final result. The BDT training for the selection of $B_s^0 \rightarrow D_s^- \pi^+$ candidates uses only the upper sideband [5466, 5800] MeV/ c^2 , as the lower sideband contains a large amount of irreducible partially reconstructed B decays, while the training for $B_s^0 \rightarrow J/\psi \phi$ uses both lower sideband [5200, 5316] MeV/ c^2 and upper mass sideband [5416, 5550] MeV/ c^2 . The B_s^0 vertex quality (χ_{vtx}^2), flight distance, momentum p , and p_T are used to discriminate the signal from the background. For the $D_s^- \pi^+$ final state we use, in addition, the χ_{vtx}^2 , flight distance, p and p_T of the D_s^- candidate and the p , p_T and χ_{IP}^2 of the bachelor pion from the B_s^0 decay to suppress combinatorial background. The quantity χ_{IP}^2 is defined as the difference in χ^2 of a given primary vertex (PV) reconstructed with and without the considered track. The training for $J/\psi \phi$ candidates uses p , p_T , χ_{vtx}^2 , and χ_{IP}^2 of the J/ψ and ϕ candidates, and the p_T of the final state kaons and muons. In the selection of B_s^0 candidates from B_c^+ decays, variables that require the candidate to point to a primary vertex, such as the impact parameter of the B_s^0 candidate, are explicitly not included. The minimum value of the BDT discriminant is chosen by optimizing the B_s^0 signal significance $S/\sqrt{S+B}$, where S and B are the expected numbers of signal and combinatorial background events, respectively.

The total number of B_s^0 decays is obtained from extended unbinned maximum likelihood fits to the invariant mass distributions, using mass constraints for the J/ψ candidates [30], and are shown in Fig. 2. The signal shapes are taken as double Crystal Ball functions [31] with a common peak value and with tails to either side of the

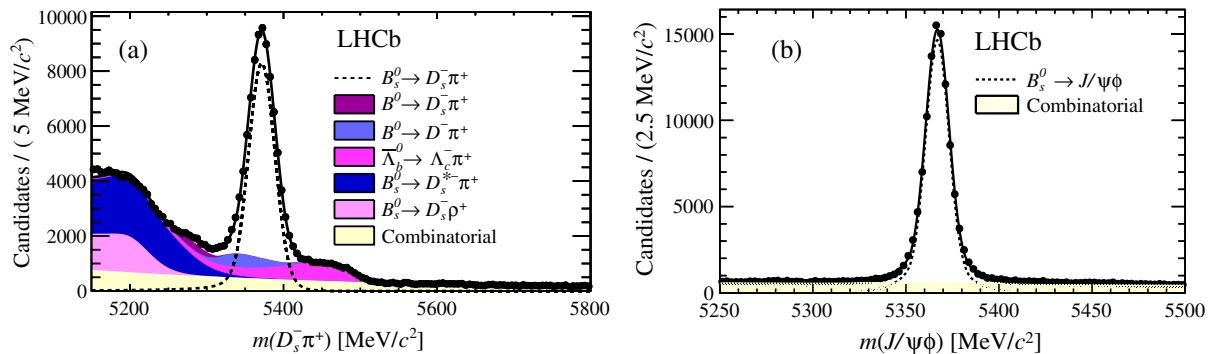


FIG. 2 (color online). Invariant mass distributions of (a) $B_s^0 \rightarrow D_s^- \pi^+$ and (b) $B_s^0 \rightarrow J/\psi \phi$ candidates. The different components are defined in the legend.

peak, to account for final state radiation and detector resolution effects. The parameters that describe the tails are obtained from simulation and are fixed in the fits. The peak and width parameters of the signal are allowed to vary. The combinatorial backgrounds are modeled with exponential distributions. The $B_s^0 \rightarrow D_s^- \pi^+$ final state is contaminated by partially reconstructed B decays such as $B_s^0 \rightarrow D_s^{*-} \pi^+$ and $B_s^0 \rightarrow D_s^- \rho^+$ decays, where the soft photon or neutral pion is not reconstructed, and by decays where one of the final state particles is misidentified as a kaon, such as $B^0 \rightarrow D^- \pi^+$ or $\bar{\Lambda}_b^0 \rightarrow \Lambda_c^- \pi^+$ decays. The shapes of these backgrounds are fixed from simulation, following Ref. [18]. In total $103\,760 \pm 380$ $B_s^0 \rightarrow J/\psi \phi$ and $73\,700 \pm 500$ $B_s^0 \rightarrow D_s^- \pi^+$ decays are found.

Selected B_s^0 candidates with masses consistent with the known B_s^0 mass are combined with tracks that satisfy loose pion identification requirements. Subsequently, B_c^+ candidates are selected with a second BDT algorithm. In the training of the second BDT, simulated candidates with masses consistent with the B_c^+ mass [32] are used as the signal, and candidates in the B_c^+ mass sideband region in data are used as the background. For this, only the upper mass sideband is used in the case of $B_s^0 \rightarrow D_s^- \pi^+$, while also the lower mass sideband is used in the case of $B_s^0 \rightarrow J/\psi \phi$, to further suppress the larger combinatorial background at smaller values of the mass. Only one sixth of the total data set is used in the training. The second BDT uses the following variables: the B_c^+ candidate p_T , decay time, χ_{vtx}^2 , χ_{IP}^2 , and the B_c^+ pointing angle, i.e., the angle between the B_c^+ candidate momentum vector and the line joining the associated PV and the B_c^+ decay vertex. The B_s^0 polar angle (the angle between B_s^0 flight direction and the beam axis), decay time, decay length, and pointing angle are also used. The p and p_T of the bachelor pion from the B_c^+ decay are the most discriminating observables in the second BDT. Differences between the analyses of the $D_s^- \pi^+$ and $J/\psi \phi$ final states are the use of χ_{IP}^2 of the B_s^0 candidate and bachelor pion (from the B_c^+ decay), and B_s^0 and B_c^+ momentum for the former, and the use of the B_c^+ and B_s^0

decay-length uncertainties for the latter. The optimal selections are defined by maximizing figures of merit for a target level of significance of 3 standard deviations, $\epsilon/(3/2 + \sqrt{B})$ [33], where ϵ is the signal efficiency for a given BDT criterion. The figure of merit displays a plateau, and the chosen value is at the lower end to allow us to better constrain the shape of the combinatorial background. The chosen selection is very close to the optimal point for a target level of 5σ and for the expected significance $S/\sqrt{S+B}$. The trigger for $B_s^0 \rightarrow D_s^- \pi^+$ decays preferentially selects candidates with high p_T with respect to the trigger for $B_s^0 \rightarrow J/\psi \phi$ decays, which results in higher efficiency for the second BDT requirement for the $B_s^0 \rightarrow D_s^- \pi^+$ final state. The B_c^+ and B_s^0 candidates are required to be produced in the pseudorapidity range $2 < \eta(B) < 5$.

The invariant mass distributions for the $B_c^+ \rightarrow B_s^0 \pi^+$ candidates are shown in Fig. 3, together with the resulting fits. The decay $B_c^+ \rightarrow B_s^0 \pi^+$ has a Q value of $770 \text{ MeV}/c^2$ (with $Q \equiv m_{B_c^+} - m_{B_s^0} - m_{\pi^+}$), which results in a resolution of about $6 \text{ MeV}/c^2$ when a B_s^0 mass constraint is applied. The signal shape is modeled as a double Crystal Ball function, with its parameters obtained from simulated events. The larger number of B_c^+ candidates in the $B_s^0 \rightarrow D_s^- \pi^+$ channel allows variation of the peak position and the width in the fit. The combinatorial background is primarily due to signal B_s^0 decays combined with a random pion from the primary vertex, and is modeled with an exponential function. Backgrounds due to $B_c^+ \rightarrow B_s^0 \pi^+$ and $B_c^+ \rightarrow B_s^0 \rho^+$ decays, where the photon or neutral pion are not reconstructed, are simulated, and their shapes are modeled with Gaussian distributions, with parameters fixed in the fit, and yields allowed to vary. Statistical signal significances of 7.7σ for $B_c^+ \rightarrow B_s^0(\rightarrow D_s^- \pi^+) \pi^+$ and 6.1σ for $B_c^+ \rightarrow B_s^0(\rightarrow J/\psi \phi) \pi^+$ decays are obtained from the likelihood ratio of fits with and without the probability density function for the signal shape, $\sqrt{-2 \ln(\mathcal{L}_B/\mathcal{L}_{S+B})}$, with 64 ± 10 and 35 ± 8 signal decays, respectively.

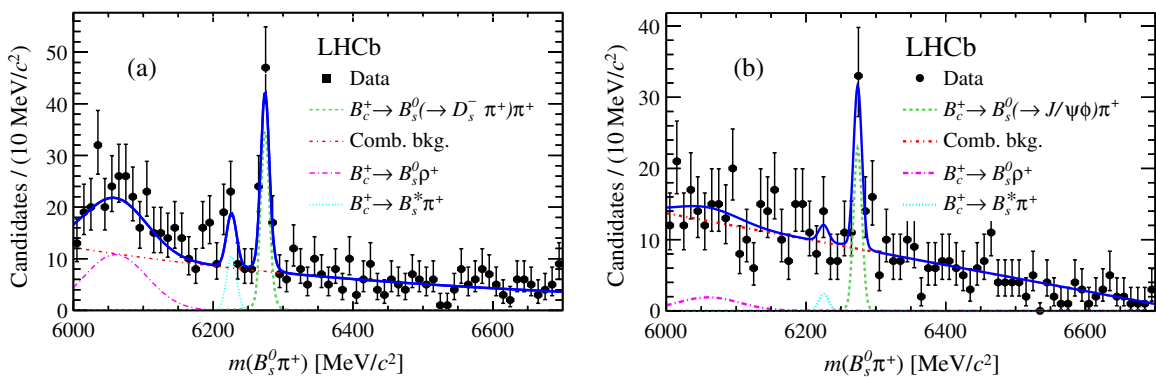


FIG. 3 (color online). B_c^+ mass fits for the combined 2011 and 2012 data sets for (a) $B_c^+ \rightarrow B_s^0(\rightarrow D_s^- \pi^+) \pi^+$ and (b) $B_c^+ \rightarrow B_s^0(\rightarrow J/\psi \phi) \pi^+$ candidates. The different components are indicated in the legends.

In Fig. 3(a), the structure around $6225 \text{ MeV}/c^2$ is consistent with originating from $B_c^+ \rightarrow B_s^* \pi^+$ decays. However, this contribution is not significant.

To obtain the value for the $B_c^+ \rightarrow B_s^0 \pi^+$ branching fraction, multiplied by the ratio of B_c^+ and B_s^0 production rates, the relative detection efficiency of B_s^0 decays compared to $B_c^+ \rightarrow B_s^0 \pi^+$ decays is determined from simulation. Requiring the bachelor pion to be inside the LHCb acceptance reduces the $B_c^+ \rightarrow B_s^0 \pi^+$ yield by about 19% with respect to the B_s^0 yield. The most significant reduction in the number of selected B_c^+ candidates comes from suppressing B_s^0 combinations with a random pion from the primary interaction, by means of the second BDT selection. The total relative detection efficiency of $B_c^+ \rightarrow B_s^0 \pi^+$ decays with respect to B_s^0 decays is estimated to be 15.2% for the $B_s^0 \rightarrow J/\psi \phi$ decay and 33.9% for the $B_s^0 \rightarrow D_s^- \pi^+$ final state. This difference in B_c^+ selection efficiencies is a consequence of the difference in B_s^0 trigger and selection requirements.

The sources of systematic uncertainty for the efficiency-corrected ratio of B_c^+ and B_s^0 yields are listed in Table I. The uncertainty on the B_s^0 yield in the $D_s^- \pi^+$ analysis is determined by varying the parameters that describe the tails of the signal mass distribution, and by reducing the exponent of the combinatorial background by a factor of 2. The uncertainty on the $B_s^0 \rightarrow J/\psi \phi$ yield is obtained by comparing the fitted yield in simulated pseudoexperiments to the yield that was used as input to those experiments.

The uncertainty on the B_c^+ yield is quantified by varying the peak position and width in the fit to $B_c^+ \rightarrow B_s^0 (\rightarrow J/\psi \phi) \pi^+$ candidates. The signal model is validated using simulated pseudoexperiments in the $J/\psi \phi$ analysis, whereas the tail parameters are varied by $\pm 10\%$ in the $D_s^- \pi^+$ analysis. In addition, the combinatorial background

TABLE I. Contributions of the various sources of (relative) systematic uncertainty on the efficiency-corrected ratio of event yields. The total systematic uncertainty is the quadratic sum of the individual contributions. The number of $B_c^+ \rightarrow B_s^0 (\rightarrow D_s^- \pi^+) \pi^+$ candidates is large enough that the peak position and width are freely varied in the fit, and hence the corresponding uncertainty is contained in the statistical uncertainty of the signal yield.

Source	$D_s^- \pi^+$ (%)	$J/\psi \phi$ (%)
B_s^0 fit model	3.0	1.2
B_c^+ mean mass	...	2.0
B_c^+ mass resolution	...	5.2
B_c^+ signal model	1.5	1.7
Combinatorial background model	1.8	0.3
Partially reconstructed background	1.8	1.7
Data-simulation difference	3.7	3.7
B_c^+ lifetime	+6.8 -3.5	7.4
Total	+8.9 -6.7	10.4

shape is changed to a straight line, and the difference in the signal yield is taken as the associated systematic uncertainty. The effect of partially reconstructed $B_c^+ \rightarrow B_s^0 \rho^+$ decays is estimated by excluding candidates with mass less than $6150 \text{ MeV}/c^2$ from the fit. The significance of the $B_c^+ \rightarrow B_s^0 \pi^+$ signal is reduced to 7.5σ for $B_c^+ \rightarrow B_s^0 (\rightarrow D_s^- \pi^+) \pi^+$ and 5.5σ for $B_c^+ \rightarrow B_s^0 (\rightarrow J/\psi \phi) \pi^+$ when the systematic uncertainties on the fit to the B_c^+ mass distribution are taken into account.

The relative detection efficiency of B_c^+ and B_s^0 events is determined from simulated events. The correspondence between data and simulation is quantified by varying the criterion on the BDT value, and by comparing the observed B_s^0 yield to the expected yield based on the change in efficiency as determined from simulation. The largest contribution is due to the 10% uncertainty on the B_c^+ lifetime [32], which was recently improved by the CDF Collaboration [34]. The change in selection efficiency when varying the B_c^+ lifetime by $\pm 10\%$ is assigned as the systematic uncertainty. A longer (shorter) B_c^+ lifetime corresponds to a larger (smaller) efficiency and therefore a smaller (larger) ratio. As a cross-check, the effect of the choice of different sets of BDT input variables is investigated and the result is found to be stable.

The contribution from Cabibbo suppressed $B_c^+ \rightarrow B_s^0 K^+$ decays, the uncertainty on the efficiency of reconstructing the extra pion, and the uncertainty on the efficiency of the particle identification requirement on the bachelor pion all give small contributions ($< 1.0\%$) to the total systematic uncertainty, and are not itemized in the summary in Table I.

The B_s^0 and B_c^+ yields are corrected for the relative detection efficiencies, to obtain the efficiency-corrected ratios of $B_c^+ \rightarrow B_s^0 \pi^+$ over B_s^0 yields, $[2.54 \pm 0.40(\text{stat})_{-0.17}^{+0.23}(\text{syst})] \times 10^{-3}$ and $[2.20 \pm 0.49(\text{stat}) \pm 0.23(\text{syst})] \times 10^{-3}$ for the $D_s^- \pi^+$ and $J/\psi \phi$ final states, respectively. The small fraction of B_s^0 candidates originating from B_c^+ decays is neglected. The uncertainty due to the uncertainty on the B_c^+ lifetime is correlated between the two measurements, and is accounted for in the combined result of the ratio of production rates multiplied with the branching fraction

$$\frac{\sigma(B_c^+)}{\sigma(B_s^0)} \times \mathcal{B}(B_c^+ \rightarrow B_s^0 \pi^+) = [2.37 \pm 0.31(\text{stat}) \pm 0.11(\text{syst})_{-0.13}^{+0.17}(\tau_{B_c^+})] \times 10^{-3},$$

where the first uncertainty is statistical, the second is systematic, and the third is due to the uncertainty on the B_c^+ lifetime. Since $\sigma(B_c^+)/\sigma(B_s^0)$ may depend on the kinematics of the produced B meson, the data are divided according to center-of-mass energy leading to $[1.27 \pm 0.42(\text{stat}) \pm 0.05(\text{syst})_{-0.07}^{+0.09}(\tau_{B_c^+})] \times 10^{-3}$ and $[2.92 \pm 0.40(\text{stat}) \pm 0.12(\text{syst})_{-0.16}^{+0.21}(\tau_{B_c^+})] \times 10^{-3}$ for $\sqrt{s} = 7$ and 8 TeV pp collisions, respectively. The lower value for the

result of the 7 TeV data is attributed to a downward statistical fluctuation of the $B_c^+ \rightarrow B_s^0(\rightarrow J/\psi\phi)\pi^+$ yield in the 2011 data set, with a p value of 1.5%.

Assuming a value for $\mathcal{B}(B_c^+ \rightarrow J/\psi\pi^+)$ around 0.15% [11], combined with the results $[\sigma(B_c^+)/\sigma(B^+)] \times \mathcal{B}(B_c^+ \rightarrow J/\psi\pi^+)/\mathcal{B}(B^+ \rightarrow J/\psi K^+) = (0.68 \pm 0.10 \pm 0.03 \pm 0.05)\%$ [4], and measurements of f_s/f_d [18] and $\mathcal{B}(B^+ \rightarrow J/\psi K^+)$ [32], results in a ratio of production rates of B_c^+ mesons over B_s^0 mesons of about 0.02. This leads to a branching fraction for $B_c^+ \rightarrow B_s^0\pi^+$ of about 10%. Although precise quantification requires improved understanding of $\sigma(B_c^+)$ and $\mathcal{B}(B_c^+ \rightarrow J/\psi\pi^+)$, even taking the lower estimates for $\mathcal{B}(B_c^+ \rightarrow J/\psi\pi^+)$ that are found in the literature [11], leads to a value of $\mathcal{B}(B_c^+ \rightarrow B_s^0\pi^+)$ which is the largest exclusive branching fraction of any known weak B meson decay.

In summary, the first observation of a weak decay of a B meson to another B meson is reported. This measurement will help to better understand flavor tagging and the decay time resolution in time-dependent B_s^0 analyses, and in addition will constrain models that predict branching fractions of B_c^+ decays.

We wish to thank A. K. Likhoded for useful discussions. We express our gratitude to our colleagues in the CERN accelerator departments for the excellent performance of the LHC. We thank the technical and administrative staff at the LHCb institutes. We acknowledge support from CERN and from the national agencies: CAPES, CNPq, FAPERJ and FINEP (Brazil); NSFC (China); CNRS/IN2P3 and Region Auvergne (France); BMBF, DFG, HGF and MPG (Germany); SFI (Ireland); INFN (Italy); FOM and NWO (The Netherlands); SCSR (Poland); MEN/IFA (Romania); MinES, Rosatom, RFBR and NRC “Kurchatov Institute” (Russia); MinECo, XuntaGal and GENCAT (Spain); SNSF and SER (Switzerland); NAS Ukraine (Ukraine); STFC (United Kingdom); NSF (USA). We also acknowledge the support received from the ERC under FP7. The Tier1 computing centers are supported by IN2P3 (France), KIT and BMBF (Germany), INFN (Italy), NWO and SURF (Netherlands), PIC (Spain), GridPP (United Kingdom). We are thankful for the computing resources put at our disposal by Yandex LLC (Russia), as well as to the communities behind the multiple open source software packages that we depend on.

[1] F. Abe *et al.* (CDF Collaboration), *Phys. Rev. Lett.* **81**, 2432 (1998); F. Abe *et al.* (CDF Collaboration), *Phys. Rev. D* **58**, 112004 (1998).
 [2] T. Aaltonen *et al.* (CDF Collaboration), *Phys. Rev. Lett.* **100**, 182002 (2008).
 [3] V.M. Abazov *et al.* (D0 Collaboration), *Phys. Rev. Lett.* **101**, 012001 (2008).
 [4] R. Aaij *et al.* (LHCb Collaboration), *Phys. Rev. Lett.* **109**, 232001 (2012).

[5] R. Aaij *et al.* (LHCb Collaboration), *Phys. Rev. Lett.* **108**, 251802 (2012).
 [6] R. Aaij *et al.* (LHCb Collaboration), *Phys. Rev. D* **87**, 071103(R) (2013).
 [7] R. Aaij *et al.* (LHCb Collaboration), *Phys. Rev. D* **87**, 112012 (2013).
 [8] R. Aaij *et al.* (LHCb Collaboration), *J. High Energy Phys.* **09** (2013) 075.
 [9] V. Kiselev, A. Kovalsky, and A. Likhoded, *Nucl. Phys.* **B585**, 353 (2000).
 [10] I.P. Gouz, V.V. Kiselev, A.K. Likhoded, V.I. Romanovsky, and O.P. Yushchenko, *Phys. At. Nucl.* **67**, 1559 (2004).
 [11] M.A. Ivanov, J.G. Korner, and P. Santorelli, *Phys. Rev. D* **73**, 054024 (2006).
 [12] A.Y. Anisimov, I. Narodetsky, C. Semay, and B. Silvestre-Brac, *Phys. Lett. B* **452**, 129 (1999).
 [13] P. Colangelo and F. De Fazio, *Phys. Rev. D* **61**, 034012 (2000).
 [14] D. Ebert, R. Faustov, and V. Galkin, *Eur. Phys. J. C* **32**, 29 (2003).
 [15] R. Dhir, N. Sharma, and R. Verma, *J. Phys. G* **35**, 085002 (2008).
 [16] Sk. Naimuddin, S. Kar, M. Priyadarsini, N. Barik, and P.C. Dash, *Phys. Rev. D* **86**, 094028 (2012).
 [17] A.A. Alves, Jr. *et al.* (LHCb Collaboration), *JINST* **3**, S08005 (2008).
 [18] R. Aaij *et al.* (LHCb Collaboration), *J. High Energy Phys.* **04** (2013) 001.
 [19] R. Aaij *et al.* (LHCb Collaboration), *Phys. Rev. D* **87**, 112010 (2013).
 [20] R. Aaij *et al.*, *JINST* **8**, P04022 (2013).
 [21] C.-H. Chang, J.-X. Wang, and X.-G. Wu, *Comput. Phys. Commun.* **174**, 241 (2006).
 [22] T. Sjöstrand, S. Mrenna, and P. Skands, *J. High Energy Phys.* **05** (2006) 026.
 [23] I. Belyaev *et al.*, in *Handling of the Generation of Primary Events in GAUSS, the LHCb Simulation Framework*, Nuclear Science Symposium Conference Record (NSS/MIC) (IEEE, New York, 2010), p. 1155.
 [24] D.J. Lange, *Nucl. Instrum. Methods Phys. Res., Sect. A* **462**, 152 (2001).
 [25] P. Golonka and Z. Was, *Eur. Phys. J. C* **45**, 97 (2006).
 [26] J. Allison *et al.* (GEANT4 Collaboration) *IEEE Trans. Nucl. Sci.* **53**, 270 (2006); S. Agostinelli *et al.* (GEANT4 Collaboration), *Nucl. Instrum. Methods Phys. Res., Sect. A* **506**, 250 (2003).
 [27] M. Clemencic, G. Corti, S. Easo, C.R. Jones, S. Miglioranza, M. Pappagallo, and P. Robbe, *J. Phys. Conf. Ser.* **331**, 032023 (2011).
 [28] L. Breiman, J.H. Friedman, R.A. Olshen, and C.J. Stone, *Classification and Regression Trees* (Wadsworth International Group, Belmont, California, USA, 1984).
 [29] R.E. Schapire and Y. Freund, *J. Comput. Syst. Sci.* **55**, 119 (1997).
 [30] W.D. Hulsbergen, *Nucl. Instrum. Methods Phys. Res., Sect. A* **552**, 566 (2005).
 [31] T. Skwarnicki, Ph.D. thesis, Institute of Nuclear Physics, Krakow, 1986, DESY-F31-86-02.

- [32] J. Beringer *et al.* (Particle Data Group), *Phys. Rev. D* **86**, 010001 (2012).
- [33] G. Punzi, in *Sensitivity of Searches for New Signals and its Optimization*, edited by L. Lyons, R. Mount, and R. Reitmeyer, Statistical Problems in Particle Physics, Astrophysics, and Cosmology, econf C030908, SLAC-R-703 (2003), p. 79.
- [34] T. Aaltonen *et al.* (CDF Collaboration), *Phys. Rev. D* **87**, 011101 (2013).

R. Aaij,⁴⁰ B. Adeva,³⁶ M. Adinolfi,⁴⁵ C. Adrover,⁶ A. Affolder,⁵¹ Z. Ajaltouni,⁵ J. Albrecht,⁹ F. Alessio,³⁷ M. Alexander,⁵⁰ S. Ali,⁴⁰ G. Alkhazov,²⁹ P. Alvarez Cartelle,³⁶ A. A. Alves, Jr.,^{24,37} S. Amato,² S. Amerio,²¹ Y. Amhis,⁷ L. Anderlini,^{17,f} J. Anderson,³⁹ R. Andreassen,⁵⁶ J. E. Andrews,⁵⁷ R. B. Appleby,⁵³ O. Aquines Gutierrez,¹⁰ F. Archilli,¹⁸ A. Artamonov,³⁴ M. Artuso,⁵⁸ E. Aslanides,⁶ G. Auriemma,^{24,m} M. Baalouch,⁵ S. Bachmann,¹¹ J. J. Back,⁴⁷ C. Baesso,⁵⁹ V. Balagura,³⁰ W. Baldini,¹⁶ R. J. Barlow,⁵³ C. Barschel,³⁷ S. Barsuk,⁷ W. Barter,⁴⁶ Th. Bauer,⁴⁰ A. Bay,³⁸ J. Beddow,⁵⁰ F. Bedeschi,²² I. Bediaga,¹ S. Belogurov,³⁰ K. Belous,³⁴ I. Belyaev,³⁰ E. Ben-Haim,⁸ G. Bencivenni,¹⁸ S. Benson,⁴⁹ J. Benton,⁴⁵ A. Berezhnoy,³¹ R. Bernet,³⁹ M.-O. Bettler,⁴⁶ M. van Beuzekom,⁴⁰ A. Bien,¹¹ S. Bifani,⁴⁴ T. Bird,⁵³ A. Bizzeti,^{17,h} P. M. Bjørnstad,⁵³ T. Blake,³⁷ F. Blanc,³⁸ J. Blouw,¹⁰ S. Blusk,⁵⁸ V. Bocci,²⁴ A. Bondar,³³ N. Bondar,²⁹ W. Bonivento,¹⁵ S. Borghi,⁵³ A. Borgia,⁵⁸ T. J. V. Bowcock,⁵¹ E. Bowen,³⁹ C. Bozzi,¹⁶ T. Brambach,⁹ J. van den Brand,⁴¹ J. Bressieux,³⁸ D. Brett,⁵³ M. Britsch,¹⁰ T. Britton,⁵⁸ N. H. Brook,⁴⁵ H. Brown,⁵¹ A. Bursche,³⁹ G. Busetto,^{21,q} J. Buytaert,³⁷ S. Cadeddu,¹⁵ O. Callot,⁷ M. Calvi,^{20,j} M. Calvo Gomez,^{35,n} A. Camboni,³⁵ P. Campana,^{18,37} D. Campora Perez,³⁷ A. Carbone,^{14,c} G. Carboni,^{23,k} R. Cardinale,^{19,i} A. Cardini,¹⁵ H. Carranza-Mejia,⁴⁹ L. Carson,⁵² K. Carvalho Akiba,² G. Casse,⁵¹ L. Cassina,¹ L. Castillo Garcia,³⁷ M. Cattaneo,³⁷ Ch. Cauet,⁹ R. Cenci,⁵⁷ M. Charles,⁵⁴ Ph. Charpentier,³⁷ P. Chen,^{3,38} S.-F. Cheung,⁵⁴ N. Chiapolini,³⁹ M. Chrzaszcz,^{39,25} K. Ciba,³⁷ X. Cid Vidal,³⁷ G. Ciezarek,⁵² P. E. L. Clarke,⁴⁹ M. Clemencic,³⁷ H. V. Cliff,⁴⁶ J. Closier,³⁷ C. Coca,²⁸ V. Coco,⁴⁰ J. Cogan,⁶ E. Cogneras,⁵ P. Collins,³⁷ A. Comerma-Montells,³⁵ A. Contu,^{15,37} A. Cook,⁴⁵ M. Coombes,⁴⁵ S. Coquereau,⁸ G. Corti,³⁷ B. Couturier,³⁷ G. A. Cowan,⁴⁹ D. C. Craik,⁴⁷ S. Cunliffe,⁵² R. Currie,⁴⁹ C. D'Ambrosio,³⁷ P. David,⁸ P. N. Y. David,⁴⁰ A. Davis,⁵⁶ I. De Bonis,⁴ K. De Bruyn,⁴⁰ S. De Capua,⁵³ M. De Cian,¹¹ J. M. De Miranda,¹ L. De Paula,² W. De Silva,⁵⁶ P. De Simone,¹⁸ D. Decamp,⁴ M. Deckenhoff,⁹ L. Del Buono,⁸ N. Deléage,⁴ D. Derkach,⁵⁴ O. Deschamps,⁵ F. Dettori,⁴¹ A. Di Canto,¹¹ H. Dijkstra,³⁷ M. Dogaru,²⁸ S. Donleavy,⁵¹ F. Dordei,¹¹ A. Dosil Suárez,³⁶ D. Dossett,⁴⁷ A. Dovbnya,⁴² F. Dupertuis,³⁸ P. Durante,³⁷ R. Dzhelyadin,³⁴ A. Dziurda,²⁵ A. Dzyuba,²⁹ S. Easo,⁴⁸ U. Egede,⁵² V. Egorychev,³⁰ S. Eidelman,³³ D. van Eijk,⁴⁰ S. Eisenhardt,⁴⁹ U. Eitschberger,⁹ R. Ekelhof,⁹ L. Eklund,^{50,37} I. El Rifai,⁵ Ch. Elsasser,³⁹ A. Falabella,^{14,e} C. Färber,¹¹ C. Farinelli,⁴⁰ S. Farry,⁵¹ D. Ferguson,⁴⁹ V. Fernandez Albor,³⁶ F. Ferreira Rodrigues,¹ M. Ferro-Luzzi,³⁷ S. Filippov,³² M. Fiore,^{16,e} C. Fitzpatrick,³⁷ M. Fontana,¹⁰ F. Fontanelli,^{19,i} R. Forty,³⁷ O. Francisco,² M. Frank,³⁷ C. Frei,³⁷ M. Frosini,^{17,37,f} E. Furfaro,^{23,k} A. Gallas Torreira,³⁶ D. Galli,^{14,c} M. Gandelman,² P. Gandini,⁵⁸ Y. Gao,³ J. Garofoli,⁵⁸ P. Garosi,⁵³ J. Garra Tico,⁴⁶ L. Garrido,³⁵ C. Gaspar,³⁷ R. Gauld,⁵⁴ E. Gersabeck,¹¹ M. Gersabeck,⁵³ T. Gershon,⁴⁷ Ph. Ghez,⁴ V. Gibson,⁴⁶ L. Giubega,²⁸ V. V. Gligorov,³⁷ C. Göbel,⁵⁹ D. Golubkov,³⁰ A. Golutvin,^{52,30,37} A. Gomes,² P. Gorbounov,^{30,37} H. Gordon,³⁷ M. Grabalosa Gándara,⁵ R. Graciani Diaz,³⁵ L. A. Granado Cardoso,³⁷ E. Graugés,³⁵ G. Graziani,¹⁷ A. Grecu,²⁸ E. Greening,⁵⁴ S. Gregson,⁴⁶ P. Griffith,⁴⁴ O. Grünberg,⁶⁰ B. Gui,⁵⁸ E. Gushchin,³² Yu. Guz,^{34,37} T. Gys,³⁷ C. Hadjivasiliou,⁵⁸ G. Haefeli,³⁸ C. Haen,³⁷ S. C. Haines,⁴⁶ S. Hall,⁵² B. Hamilton,⁵⁷ T. Hampson,⁴⁵ S. Hansmann-Menzemer,¹¹ N. Harnew,⁵⁴ S. T. Harnew,⁴⁵ J. Harrison,⁵³ T. Hartmann,⁶⁰ J. He,³⁷ T. Head,³⁷ V. Heijne,⁴⁰ K. Hennessy,⁵¹ P. Henrard,⁵ J. A. Hernando Morata,³⁶ E. van Herwijnen,³⁷ M. Heß,⁶⁰ A. Hicheur,¹ E. Hicks,⁵¹ D. Hill,⁵⁴ M. Hoballah,⁵ C. Hombach,⁵³ W. Hulsbergen,⁴⁰ P. Hunt,⁵⁴ T. Huse,⁵¹ N. Hussain,⁵⁴ D. Hutchcroft,⁵¹ D. Hynds,⁵⁰ V. Iakovenko,⁴³ M. Idzik,²⁶ P. Ilten,¹² R. Jacobsson,³⁷ A. Jaeger,¹¹ E. Jans,⁴⁰ P. Jatun,³⁸ A. Jawahery,⁵⁷ F. Jing,³ M. John,⁵⁴ D. Johnson,⁵⁴ C. R. Jones,⁴⁶ C. Joram,³⁷ B. Jost,³⁷ M. Kabbalo,⁹ S. Kandybei,⁴² W. Kanso,⁶ M. Karacson,³⁷ T. M. Karbach,³⁷ I. R. Kenyon,⁴⁴ T. Ketel,⁴¹ B. Khanji,²⁰ O. Kochebina,⁷ I. Komarov,³⁸ R. F. Koopman,⁴¹ P. Koppenburg,⁴⁰ M. Korolev,³¹ A. Kozlinskiy,⁴⁰ L. Kravchuk,³² K. Kreplin,¹¹ M. Kreps,⁴⁷ G. Krocker,¹¹ P. Krokovny,³³ F. Kruse,⁹ M. Kucharczyk,^{20,25,37,j} V. Kudryavtsev,³³ K. Kurek,²⁷ T. Kvaratskheliya,^{30,37} V. N. La Thi,³⁸ D. Lacarrere,³⁷ G. Lafferty,⁵³ A. Lai,¹⁵ D. Lambert,⁴⁹ R. W. Lambert,⁴¹ E. Lanciotti,³⁷ G. Lanfranchi,¹⁸ C. Langenbruch,³⁷ T. Latham,⁴⁷ C. Lazzeroni,⁴⁴ R. Le Gac,⁶ J. van Leerdam,⁴⁰ J.-P. Lees,⁴ R. Lefèvre,⁵ A. Leflat,³¹ J. Lefrançois,⁷ S. Leo,²² O. Leroy,⁶ T. Lesiak,²⁵ B. Leverington,¹¹ Y. Li,³ L. Li Gioi,⁵ M. Liles,⁵¹ R. Lindner,³⁷ C. Linn,¹¹ B. Liu,³ G. Liu,³⁷ S. Lohn,³⁷ I. Longstaff,⁵⁰ J. H. Lopes,² N. Lopez-March,³⁸ H. Lu,³ D. Lucchesi,^{21,q} J. Luisier,³⁸ H. Luo,⁴⁹ O. Lupton,⁵⁴ F. Machefert,⁷ I. V. Machikhiliyan,^{4,30} F. Maciuc,²⁸ O. Maev,^{29,37} S. Malde,⁵⁴

G. Manca,^{15,d} G. Mancinelli,⁶ J. Maratas,⁵ U. Marconi,¹⁴ P. Marino,^{22,s} R. Märki,³⁸ J. Marks,¹¹ G. Martellotti,²⁴ A. Martens,⁸ A. Martín Sánchez,⁷ M. Martinelli,⁴⁰ D. Martinez Santos,^{41,37} D. Martins Tostes,² A. Martynov,³¹ A. Massafferri,¹ R. Matev,³⁷ Z. Mathe,³⁷ C. Matteuzzi,²⁰ E. Maurice,⁶ A. Mazurov,^{16,32,37,e} J. McCarthy,⁴⁴ A. McNab,⁵³ R. McNulty,¹² B. McSkelly,⁵¹ B. Meadows,^{56,54} F. Meier,⁹ M. Meissner,¹¹ M. Merk,⁴⁰ D. A. Milanes,⁸ M.-N. Minard,⁴ J. Molina Rodriguez,⁵⁹ S. Monteil,⁵ D. Moran,⁵³ P. Morawski,²⁵ A. Mordà,⁶ M. J. Morello,^{22,s} R. Mountain,⁵⁸ I. Mous,⁴⁰ F. Muheim,⁴⁹ K. Müller,³⁹ R. Muresan,²⁸ B. Muryn,²⁶ B. Muster,³⁸ P. Naik,⁴⁵ T. Nakada,³⁸ R. Nandakumar,⁴⁸ I. Nasteva,¹ M. Needham,⁴⁹ S. Neubert,³⁷ N. Neufeld,³⁷ A. D. Nguyen,³⁸ T. D. Nguyen,³⁸ C. Nguyen-Mau,^{38,o} M. Nicol,⁷ V. Niess,⁵ R. Niet,⁹ N. Nikitin,³¹ T. Nikodem,¹¹ A. Nomerotski,⁵⁴ A. Novoselov,³⁴ A. Oblakowska-Mucha,²⁶ V. Obraztsov,³⁴ S. Oggero,⁴⁰ S. Ogilvy,⁵⁰ O. Okhrimenko,⁴³ R. Oldeman,^{15,d} M. Orlandea,²⁸ J. M. Otalora Goicochea,² P. Owen,⁵² A. Oyanguren,³⁵ B. K. Pal,⁵⁸ A. Palano,^{13,b} M. Palutan,¹⁸ J. Panman,³⁷ A. Papanestis,⁴⁸ M. Pappagallo,⁵⁰ C. Parkes,⁵³ C. J. Parkinson,⁵² G. Passaleva,¹⁷ G. D. Patel,⁵¹ M. Patel,⁵² G. N. Patrick,⁴⁸ C. Patrignani,^{19,i} C. Pavel-Nicorescu,²⁸ A. Pazos Alvarez,³⁶ A. Pearce,⁵³ A. Pellegrino,⁴⁰ G. Penso,^{24,l} M. Pepe Altarelli,³⁷ S. Perazzini,^{14,c} E. Perez Trigo,³⁶ A. Pérez-Calero Yzquierdo,³⁵ P. Perret,⁵ M. Perrin-Terrin,⁶ L. Pescatore,⁴⁴ E. Pesen,⁶¹ G. Pessina,²⁰ K. Petridis,⁵² A. Petrolini,^{19,i} A. Phan,⁵⁸ E. Picatoste Olloqui,³⁵ B. Pietrzyk,⁴ T. Pilař,⁴⁷ D. Pinci,²⁴ S. Playfer,⁴⁹ M. Plo Casasus,³⁶ F. Polci,⁸ G. Polok,²⁵ A. Poluektov,^{47,33} E. Polycarpo,² A. Popov,³⁴ D. Popov,¹⁰ B. Popovici,²⁸ C. Potterat,³⁵ A. Powell,⁵⁴ J. Prisciandaro,³⁸ A. Pritchard,⁵¹ C. Prouve,⁷ V. Pugatch,⁴³ A. Puig Navarro,³⁸ G. Punzi,^{22,r} W. Qian,⁴ J. H. Rademacker,⁴⁵ B. Rakotomiramanana,³⁸ M. S. Rangel,² I. Raniuk,⁴² N. Rauschmayr,³⁷ G. Raven,⁴¹ S. Redford,⁵⁴ M. M. Reid,⁴⁷ A. C. dos Reis,¹ S. Ricciardi,⁴⁸ A. Richards,⁵² K. Rinnert,⁵¹ V. Rives Molina,³⁵ D. A. Roa Romero,⁵ P. Robbe,⁷ D. A. Roberts,⁵⁷ A. B. Rodrigues,¹ E. Rodrigues,⁵³ P. Rodriguez Perez,³⁶ S. Roiser,³⁷ V. Romanovsky,³⁴ A. Romero Vidal,³⁶ J. Rouvinet,³⁸ T. Ruf,³⁷ F. Ruffini,²² H. Ruiz,³⁵ P. Ruiz Valls,³⁵ G. Sabatino,^{24,k} J. J. Saborido Silva,³⁶ N. Sagidova,²⁹ P. Sail,⁵⁰ B. Saitta,^{15,d} V. Salustino Guimaraes,² B. Sanmartin Sedes,³⁶ R. Santacesaria,²⁴ C. Santamarina Rios,³⁶ E. Santovetti,^{23,k} M. Sapunov,⁶ A. Sarti,¹⁸ C. Satriano,^{24,m} A. Satta,²³ M. Savrie,^{16,e} D. Savrina,^{30,31} M. Schiller,⁴¹ H. Schindler,³⁷ M. Schlupp,⁹ M. Schmelling,¹⁰ B. Schmidt,³⁷ O. Schneider,³⁸ A. Schopper,³⁷ M.-H. Schune,⁷ R. Schwemmer,³⁷ B. Sciascia,¹⁸ A. Sciubba,²⁴ M. Seco,³⁶ A. Semennikov,³⁰ K. Senderowska,²⁶ I. Sepp,⁵² N. Serra,³⁹ J. Serrano,⁶ P. Seyfert,¹¹ M. Shapkin,³⁴ I. Shapoval,^{16,42,e} P. Shatalov,³⁰ Y. Shcheglov,²⁹ T. Shears,⁵¹ L. Shekhtman,³³ O. Shevchenko,⁴² V. Shevchenko,³⁰ A. Shires,⁹ R. Silva Coutinho,⁴⁷ M. Sirendi,⁴⁶ N. Skidmore,⁴⁵ T. Skwarnicki,⁵⁸ N. A. Smith,⁵¹ E. Smith,^{54,48} E. Smith,⁵² J. Smith,⁴⁶ M. Smith,⁵³ M. D. Sokoloff,⁵⁶ F. J. P. Soler,⁵⁰ F. Soomro,³⁸ D. Souza,⁴⁵ B. Souza De Paula,² B. Spaan,⁹ A. Sparkes,⁴⁹ P. Spradlin,⁵⁰ F. Stagni,³⁷ S. Stahl,¹¹ O. Steinkamp,³⁹ S. Stevenson,⁵⁴ S. Stoica,²⁸ S. Stone,⁵⁸ B. Storaci,³⁹ M. Straticiu,²⁸ U. Straumann,³⁹ V. K. Subbiah,³⁷ L. Sun,⁵⁶ W. Sutcliffe,⁵² S. Swientek,⁹ V. Syropoulos,⁴¹ M. Szczekowski,²⁷ P. Szczypka,^{38,37} D. Szilard,² T. Szumlak,²⁶ S. T'Jampens,⁴ M. Teklishyn,⁷ E. Teodorescu,²⁸ F. Teubert,³⁷ C. Thomas,⁵⁴ E. Thomas,³⁷ J. van Tilburg,¹¹ V. Tisserand,⁴ M. Tobin,³⁸ S. Tolk,⁴¹ D. Tonelli,³⁷ S. Topp-Joergensen,⁵⁴ N. Torr,⁵⁴ E. Tournefier,^{4,52} S. Tourneur,³⁸ M. T. Tran,³⁸ M. Tresch,³⁹ A. Tsaregorodtsev,⁶ P. Tsopelas,⁴⁰ N. Tuning,^{40,37} M. Ubeda Garcia,³⁷ A. Ukleja,²⁷ A. Ustyuzhanin,^{52,p} U. Uwer,¹¹ V. Vagnoni,¹⁴ G. Valenti,¹⁴ A. Vallier,⁷ R. Vazquez Gomez,¹⁸ P. Vazquez Regueiro,³⁶ C. Vázquez Sierra,³⁶ S. Vecchi,¹⁶ J. J. Velthuis,⁴⁵ M. Veltri,^{17,g} G. Veneziano,³⁸ M. Vesterinen,³⁷ B. Viaud,⁷ D. Vieira,² X. Vilasis-Cardona,^{35,n} A. Vollhardt,³⁹ D. Volyanskyy,¹⁰ D. Voong,⁴⁵ A. Vorobyev,²⁹ V. Vorobyev,³³ C. Voß,⁶⁰ H. Voss,¹⁰ J. A. de Vries,⁴⁰ R. Waldi,⁶⁰ C. Wallace,⁴⁷ R. Wallace,¹² S. Wandernoth,¹¹ J. Wang,⁵⁸ D. R. Ward,⁴⁶ N. K. Watson,⁴⁴ A. D. Webber,⁵³ D. Websdale,⁵² M. Whitehead,⁴⁷ J. Wicht,³⁷ J. Wiechczynski,²⁵ D. Wiedner,¹¹ L. Wiggers,⁴⁰ G. Wilkinson,⁵⁴ M. P. Williams,^{47,48} M. Williams,⁵⁵ F. F. Wilson,⁴⁸ J. Wimberley,⁵⁷ J. Wishahi,⁹ W. Wislicki,²⁷ M. Witek,²⁵ S. A. Wotton,⁴⁶ S. Wright,⁴⁶ S. Wu,³ K. Wyllie,³⁷ Y. Xie,^{49,37} Z. Xing,⁵⁸ Z. Yang,³ X. Yuan,³ O. Yushchenko,³⁴ M. Zangoli,¹⁴ M. Zavertyaev,^{10,a} F. Zhang,³ L. Zhang,⁵⁸ W. C. Zhang,¹² Y. Zhang,³ A. Zhelezov,¹¹ A. Zhokhov,³⁰ L. Zhong,³ and A. Zvyagin³⁷

(LHCb Collaboration)

¹Centro Brasileiro de Pesquisas Físicas (CBPF), Rio de Janeiro, Brazil²Universidade Federal do Rio de Janeiro (UFRJ), Rio de Janeiro, Brazil³Center for High Energy Physics, Tsinghua University, Beijing, China⁴LAPP, Université de Savoie, CNRS/IN2P3, Annecy-Le-Vieux, France⁵Clermont Université, Université Blaise Pascal, CNRS/IN2P3, LPC, Clermont-Ferrand, France

- ⁶CPPM, Aix-Marseille Université, CNRS/IN2P3, Marseille, France
⁷LAL, Université Paris-Sud, CNRS/IN2P3, Orsay, France
⁸LPNHE, Université Pierre et Marie Curie, Université Paris Diderot, CNRS/IN2P3, Paris, France
⁹Fakultät Physik, Technische Universität Dortmund, Dortmund, Germany
¹⁰Max-Planck-Institut für Kernphysik (MPIK), Heidelberg, Germany
¹¹Physikalisches Institut, Ruprecht-Karls-Universität Heidelberg, Heidelberg, Germany
¹²School of Physics, University College Dublin, Dublin, Ireland
¹³Sezione INFN di Bari, Bari, Italy
¹⁴Sezione INFN di Bologna, Bologna, Italy
¹⁵Sezione INFN di Cagliari, Cagliari, Italy
¹⁶Sezione INFN di Ferrara, Ferrara, Italy
¹⁷Sezione INFN di Firenze, Firenze, Italy
¹⁸Laboratori Nazionali dell'INFN di Frascati, Frascati, Italy
¹⁹Sezione INFN di Genova, Genova, Italy
²⁰Sezione INFN di Milano Bicocca, Milano, Italy
²¹Sezione INFN di Padova, Padova, Italy
²²Sezione INFN di Pisa, Pisa, Italy
²³Sezione INFN di Roma Tor Vergata, Roma, Italy
²⁴Sezione INFN di Roma La Sapienza, Roma, Italy
²⁵Henryk Niewodniczanski Institute of Nuclear Physics Polish Academy of Sciences, Kraków, Poland
²⁶AGH - University of Science and Technology, Faculty of Physics and Applied Computer Science, Kraków, Poland
²⁷National Center for Nuclear Research (NCBJ), Warsaw, Poland
²⁸Horia Hulubei National Institute of Physics and Nuclear Engineering, Bucharest-Magurele, Romania
²⁹Petersburg Nuclear Physics Institute (PNPI), Gatchina, Russia
³⁰Institute of Theoretical and Experimental Physics (ITEP), Moscow, Russia
³¹Institute of Nuclear Physics, Moscow State University (SINP MSU), Moscow, Russia
³²Institute for Nuclear Research of the Russian Academy of Sciences (INR RAN), Moscow, Russia
³³Budker Institute of Nuclear Physics (SB RAS) and Novosibirsk State University, Novosibirsk, Russia
³⁴Institute for High Energy Physics (IHEP), Protvino, Russia
³⁵Universitat de Barcelona, Barcelona, Spain
³⁶Universidad de Santiago de Compostela, Santiago de Compostela, Spain
³⁷European Organization for Nuclear Research (CERN), Geneva, Switzerland
³⁸Ecole Polytechnique Fédérale de Lausanne (EPFL), Lausanne, Switzerland
³⁹Physik-Institut, Universität Zürich, Zürich, Switzerland
⁴⁰Nikhef National Institute for Subatomic Physics, Amsterdam, The Netherlands
⁴¹Nikhef National Institute for Subatomic Physics and VU University Amsterdam, Amsterdam, The Netherlands
⁴²NSC Kharkiv Institute of Physics and Technology (NSC KIPT), Kharkiv, Ukraine
⁴³Institute for Nuclear Research of the National Academy of Sciences (KINR), Kyiv, Ukraine
⁴⁴University of Birmingham, Birmingham, United Kingdom
⁴⁵H. H. Wills Physics Laboratory, University of Bristol, Bristol, United Kingdom
⁴⁶Cavendish Laboratory, University of Cambridge, Cambridge, United Kingdom
⁴⁷Department of Physics, University of Warwick, Coventry, United Kingdom
⁴⁸STFC Rutherford Appleton Laboratory, Didcot, United Kingdom
⁴⁹School of Physics and Astronomy, University of Edinburgh, Edinburgh, United Kingdom
⁵⁰School of Physics and Astronomy, University of Glasgow, Glasgow, United Kingdom
⁵¹Oliver Lodge Laboratory, University of Liverpool, Liverpool, United Kingdom
⁵²Imperial College London, London, United Kingdom
⁵³School of Physics and Astronomy, University of Manchester, Manchester, United Kingdom
⁵⁴Department of Physics, University of Oxford, Oxford, United Kingdom
⁵⁵Massachusetts Institute of Technology, Cambridge, Massachusetts, USA
⁵⁶University of Cincinnati, Cincinnati, Ohio, USA
⁵⁷University of Maryland, College Park, Maryland, USA
⁵⁸Syracuse University, Syracuse, New York, USA
⁵⁹Pontifícia Universidade Católica do Rio de Janeiro (PUC-Rio), Rio de Janeiro, Brazil [associated with Universidade Federal do Rio de Janeiro (UFRJ), Rio de Janeiro, Brazil]
⁶⁰Institut für Physik, Universität Rostock, Rostock, Germany (associated with Physikalisches Institut, Ruprecht-Karls-Universität Heidelberg, Heidelberg, Germany)
⁶¹Celal Bayar University, Manisa, Turkey [associated with European Organization for Nuclear Research (CERN), Geneva, Switzerland]

^aAlso at P.N. Lebedev Physical Institute, Russian Academy of Science (LPI RAS), Moscow, Russia.

^bAlso at Università di Bari, Bari, Italy.

^cAlso at Università di Bologna, Bologna, Italy.

^dAlso at Università di Cagliari, Cagliari, Italy.

^eAlso at Università di Ferrara, Ferrara, Italy.

^fAlso at Università di Firenze, Firenze, Italy.

^gAlso at Università di Urbino, Urbino, Italy.

^hAlso at Università di Modena e Reggio Emilia, Modena, Italy.

ⁱAlso at Università di Genova, Genova, Italy.

^jAlso at Università di Milano Bicocca, Milano, Italy.

^kAlso at Università di Roma Tor Vergata, Roma, Italy.

^lAlso at Università di Roma La Sapienza, Roma, Italy.

^mAlso at Università della Basilicata, Potenza, Italy.

ⁿAlso at LIFAELS, La Salle, Universitat Ramon Llull, Barcelona, Spain.

^oAlso at Hanoi University of Science, Hanoi, Vietnam.

^pAlso at Institute of Physics and Technology, Moscow, Russia.

^qAlso at Università di Padova, Padova, Italy.

^rAlso at Università di Pisa, Pisa, Italy.

^sAlso at Scuola Normale Superiore, Pisa, Italy.